A R C H I V E S O F M E T A L L U R G Y A N D M A T E R I A L S
Volume 50 2005 Issue 4

M. SATERNUS*, J. BOTOR*, W. WĘŻYK**, T. STUCZYŃSKI**

THE HYDRODYNAMIC OF THE SYSTEM: LIQUID ALUMINIUM ALLOY — REFINING GAS

HYDRODYNAMIKA W UKŁADZIE: CIEKŁY STOP ALUMINIUM — GAZ RAFINUJĄCY

The influence of the flow rate of refining gas on the bubble creation process and the bubble shape was presented. Schemes of gas dispersion in liquid metal in comparison with the model data were shown. The influence of the flow rate of refining gas on the hydrogen removal process from aluminium (final hydrogen concentration) was presented taking into consideration the refining process of AlSi7Mg alloy. The equivalent bubble diameter was presented. Basing on this equation the calculation of bubble diameter, average bubble diameter and optimal refining time was done.

W pracy przedstawiono wpływ natężenia przepływu gazu na proces tworzenia się pęcherzyków gazowych oraz kształt tychże pęcherzyków. Przedstawiono cztery różne schematy przepływu gazu w ciekłym metalu i ich stopień dyspersji. Modele te zestawiono z wynikami badań doświadczalnych przeprowadzonych w IMN — OML w Skawinie. Wpływ natężenia przepływu gazu na proces usuwania wodoru z aluminium (stężenie wodoru po procesie rafinacji) przedstawiono dla wyników uzyskanych w procesie rafinacji stopu AlSi7Mg. Przedstawiono równanie pozwalające wyliczyć wielkość optymalnego czasu rafinacji średnicy pęcherzyków gazowych dla danego procesu rafinacji w zależności od natężenia przepływu gazu rafinującego oraz średniej średnicy pęcherzyków gazowych.

1. Introduction

In metallurgy the quality of the liquid metal has the biggest influence on the quality of the final products. The amount of metallic and non-metallic impurities has great impact on the next stages of technological processes like casting, plastic working, heat

* POLITECHNIKA ŚLĄSKA, 40-085 KATOWICE, UL. KRASIŃSKIEGO 8
** IMN-OML, 32-050 SKAWINA, UL. PIŁSUDSKIEGO 19

treatment, etc. Because of this the refining process is considered to be one of the basic technological stages.

In the metallurgical industry, and especially in aluminium production the barbotage method of refining process is very popular and this method can be the leading one [1, 2]. Today the most popular are refining reactors with impellers which can generate small gas bubbles. A rotary impeller causes also the metal bath to be stirred well. There are two basic hydrodynamics parameters: the flow rate of refining gas and the mixing of refining gas (due to the rotor action) that influences good stirring of metal and generation of small gas bubbles. For this reason the studies on the hydrodynamic conditions of system: liquid metal/alloys — refining gas are of considerable value.

2. Hydrodynamics of barbotage

The flow rate of refining gas influences on the shape of gas bubbles and on the process of their creation. The Figure 1 shows the influence of flow rate of refining gas

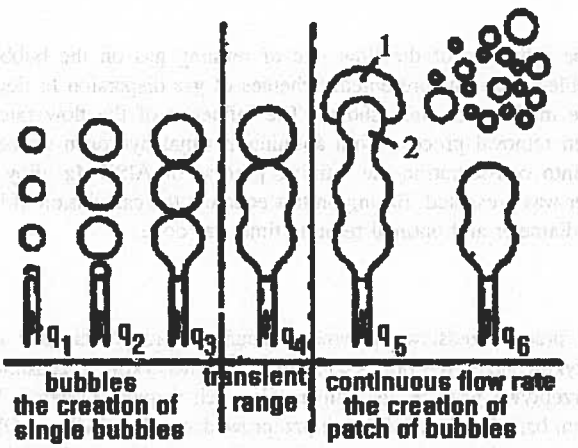

Fig. 1. The influence of the flow rate of refining gas on the bubble creation process [3]

on the process of gas bubble creation. In the range q_1 to q_3 we can observe the free movement of gas bubbles. When the flow reaches the limiting value q_3 we observe the creation of bubble chain and then the space between bubbles disappears and bubbles can be deformed. The flow rate equal to (q_4) causes that the films between bubbles are broken. After reaching value q_5 and q_6 bubble 1 hits bubble 2 and then we can observe their disintegration. Thus the creation of patch of bubbles that have different diameters is possible. Gas bubbles and liquid drops moving in the liquid phase have the determined shapes. We can distinguish the six different shapes (Fig. 2a):

1. spherical,
2. ellipsoidal,
3. dimpled ellipsoidal cap,

4. skirted,
5. spherical cap,
6. wobbling.

Fig. 2 shows the regimes of persistence of determined shape of bubbles or drops depending on physicochemical properties (density, surface tension, viscosity) and hydrodynamic conditions (flow rate of refining gas, nozzle diameter).

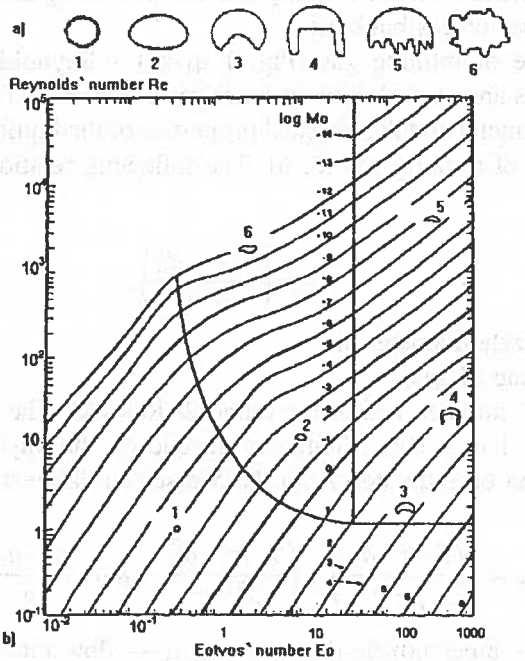

Fig. 2. a) Shapes of gas bubbles and liquids drops moving in liquid phase, b) regimes of persistence of determined shape of these bubbles and drops 1 — spherical, 2 — ellipsoidal, 3 — dimpled ellipsoidal cap, 4 — skirted, 5 — spherical cap, 6 — wobbling [4]

The analysis of shapes of gas bubbles presented in Fig. 2 leads to conclusion that it is necessary to introduce the equivalent bubble diameter d_e. It is the diameter which the bubble would have if it was a spherical one. The equivalent diameter is described by three criterial numbers:

▷ Reynolds' number Re,

▷ Eotvos' number Eo:

$$Eo = (g \cdot \Delta\rho \cdot d_e^2)/\sigma \qquad (1)$$

▷ Morton's number Mo:

$$Mo = (g \cdot \eta^4 \cdot \Delta\rho)/(\rho^2 \cdot \sigma^3), \tag{2}$$

where: g — gravitational constant, m/s^2, ρ — density of liquid metals, kg/m^3, σ — surface tension of liquid metals, N/m, d_e — equivalent gas bubble diameter, m, η — viscosity of liquids, Pa·s.

Three main ranges of flow rate of refining gas can be distinguished, which correspond to the different shapes of gas bubbles:

1. At low flow rate of refining gas (Fig. 1 q_1-q_2) – Reynolds' number Re<2, the spherical bubbles are created without inner gas circulation. Their diameter depends on the nozzle diameter and the physical properties of the liquids and are independent on the flow rate of refining gas [5, 6]. The following relationship is valid for this range [7, 8]:

$$d_e = \left(\frac{6 \cdot \sigma \cdot d_d}{\rho \cdot g}\right), \tag{3}$$

   where: d_d — nozzle diameter, m.

2. Moderate flow rate of gas:
   a) At Reynolds' number within the range 2<Re<400. The spherical bubbles are formed (Fig. 1 q_3). Their diameters depend on the physical properties of the liquid and can be estimated from the Mersen's relationship [9]:

$$d_e = \left\{\left(\frac{3 \cdot \sigma \cdot d_w}{\rho \cdot g}\right) + \left(\frac{9 \cdot \sigma^2 \cdot d_w^2}{\rho^2 \cdot g^2} + K_M \cdot \frac{q^2 \cdot d_w}{g}\right)^{0.5}\right\}^{0.333}, \tag{4}$$

      where: d_w — inner nozzle diameter, m, q — flow rate of refining gas, m^3/s, K_M — a constant.

   b) Reynolds' number: 400<Re<5000. In this range bubbles become deformed under the action of liquid phase drag forces and take the shape of skirted or spherical caps (Fig. 1 q_4 and q_5). The equivalent bubble diameter can be determined from Davidson's and Amick's relationship [10]:

$$d_e = 0.54 \cdot \left(q \cdot \sqrt{d_d}\right)^{0.289}. \tag{5}$$

3. High flow rate of refining gas (Fig. 1 q_5 and q_6), Reynolds' number larger than 5000. Shortly after leaving the nozzle exit the bubbles merge to create the chain and the space between them is reduced. The shape of bubbles remains the spherical, the equivalent diameter depends on the flow rate of refining gas and is independent on the nozzle diameter and the physical properties of the liquids. The equivalent bubble diameter in this range can be determined after Leibson's et al. relationship [11, 12]:

$$d_e \cong 0.71 \cdot \mathrm{Re}^{-0.mk05}. \tag{6}$$

For the moderate flow rate of refining gas the equivalent bubble diameter, which is in range 0.005 to 0.015 m — is dependent only on the flow rate of refining gas. Bubbles of very small diameter (0.005–0.007 m) are mostly spherical one (Fig. 2.1). When the flow rate of refining gas is risen up bubbles diameter is between 0.008-0.010 m and they are ellipsoidal (Fig. 2.2) or dimpled ellipsoidal cap (Fig. 2.3). The shape of spherical cap (Fig. 2.5) is typical for bubbles which diameter is larger than 0.010. If bubbles diameter is still rising up shape of bubbles would be wobbling (Fig. 2.4, 2.6), and the chain flow is possible (Fig. 1 q_5, q_6).

The reactors with impellers generate small gas bubbles ranging from 0.005 m to 0.015 m. In small bubbles the surface film is motionless and they move their linearly. In larger bubbles the inner circulation of gas is observed, which causes the rise of gas velocity. The scheme of this phenomenon is presented in Fig. 3.

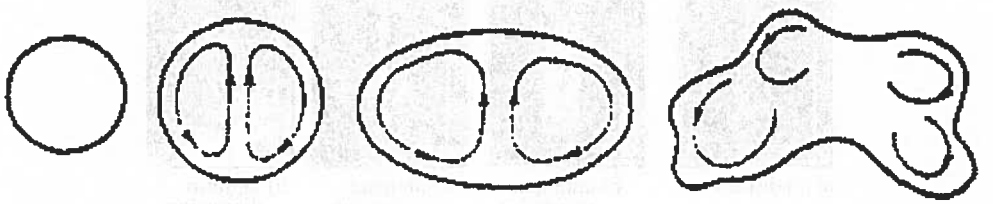

Fig. 3. The inner circulation in gas bubble [3]

3. Physical model

Fig. 4 presents four different flow patterns of gas bubbles in liquid metals classified by Oldshue [13] and the corresponding ratios of dispersion. In the process of hydrogen removal from liquid aluminium the gas bubbles generated in reactors with impellers can be uniformly dispersed in whole volume of metal (Fig. 4d). This can lead to the low level of impurities and shorter time of degassing. That can be effected when we choose the right process parameters, mainly the rotation speed and the flow rate of refining gas.

Fig. 5 shows examples of results obtained in the study, where water models were used for checking the dispersion of gases and effectiveness of the oxygen removal from water. This is an analogy to the hydrogen desorption from aluminium. These research was done in IMN — OML in Skawina [14]. The size of the experimental chamber are the same (diameter 0,5 m, height 0,7 m) as the industrial melting crucible.

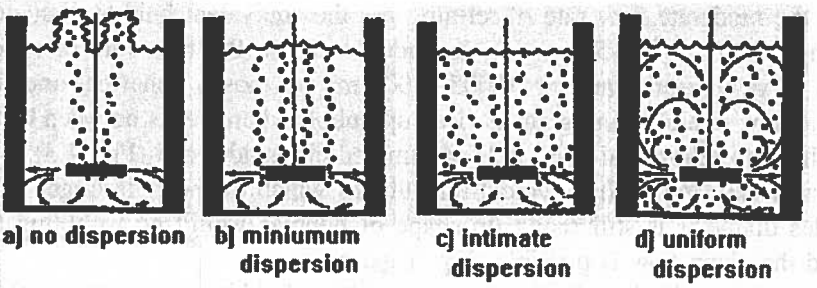

Fig. 4. Flow pattern of gas bubbles in liquid metals and their ratio of dispersion [13]

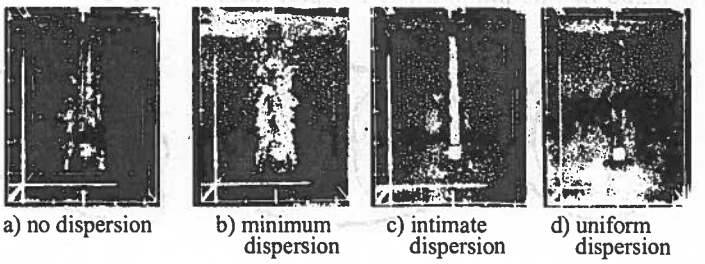

Fig. 5. The ratio of refining gas dispersion in liquid aluminium (modeling researches) a) q = 5 dm^3/min, no rotor rotation; b) q = 25 dm^3/min, no rotor rotation; c) q = 2 dm^3/min, rotor rotation: 250 rpm; d0 q = 5 dm^3/min, rotor rotation: 350 rpm [14]

4. Mathematical model

For the system: hydrogen dissolved in liquid aluminium — purging gas the laboratory studies were carried out [15, 5, 16] as well as the experiments of refining process in industrial conditions [1, 2]. In both cases it was found that the hydrogen degassing from liquid aluminium by purging gases has a diffusional character i.e. is controlled by mass transport in the liquid metallic phase. Using the available mathematical models for the description of this process [1, 2, 17, 18] the equation for calculation the final hydrogen concentration after refining in batch reactors can be written in following form:

$$\frac{c_t}{c_i} = \exp\left(-\frac{k \cdot \rho \cdot A}{M} \cdot t\right), \tag{7}$$

where: t — refining time, s, k — mass transfer coefficient, m/s, ρ — density of liquid aluminium, kg/m^3, A — interfacial contact area of bubbles in melt, m^2, c_t — final hydrogen concentration after degassing, % mas., c_i — initial hydrogen concentration, % mas., M — mass of liquid melt, kg.

In the analysis of hydrogen degassing process it is essential to estimate the value of the interfacial contact area. For the spherical cap rising up from the single nozzle we can use the following equation:

$$A = \frac{6 \cdot q \cdot h}{u \cdot d}, \tag{8}$$

where: h — height of liquid aluminium, m, u — bubble rise velocity, m/s, d — gas bubble diameter, m.

To calculate the interfacial contact area for gas bubbles of different shapes we can use complex relationships [19, 20]. However, this procedure requires many data which are difficult to estimate. In the industrial reactors the gas is as a rule introduced to aluminium by rotors (rotating nozzle). This cause that gas bubbles are very well mixed with liquid metal and this fact let many authors [5, 17, 18, 21, 22] use the equation (8) to calculate the interfacial contact area. Because the shape of gas bubble are different, the equivalent bubble diameter is introduced to this equation. The surface area at the top of the melt can be neglected because of fact that: the values of the interfacial contact area of bubbles in melt and mass transfer coefficient on the boundary: bubble — metal phase are significantly higher than at the surface area at the top of the melt, the driver force of process at the surface area at the top of the melt is significantly smaller than on the boundary: bubble — metal phase. This assumption was verified by the laboratory experiments and industrial observation [23].

In the mathematical description of hydrogen degassing from liquid aluminium one needs to know relationships for density of liquid aluminium ρ, mass transfer coefficient k and the gas bubble rise velocity u. The analysis and selection of these parameters were done in earlier works [1, 2], and the following relationships were deduced:

a) density of the liquid alloy:

$$\rho = 2.368 - 2.63 \cdot 10^{-4} \cdot (T - T_p) \tag{9}$$

b) gas bubble rise velocity:

$$u = 1.02 \sqrt{\frac{g \cdot d_e}{2}} \tag{10}$$

c) mass transfer coefficient:

$$k = 0.0122 \cdot e^{-24685.6/(R \cdot T)} \cdot (d_e/1.37)^{-0.25}, \tag{11}$$

where: T_p — temperature of melting, K, g — gravitational constant, m/s^2, R — gas constant, J/K.mol.

To estimate the equivalent gas bubble diameter we assume that the volume of refining gas which is introduced to reactor is constant:

$$V = q \cdot t = \text{constant}. \tag{12}$$

This means that in case of 10 minutes refining period the following gas volumes are obtained for corresponding flow rates:
a) q =10 l/min → V = 0.1002 m^3
b) q =15 l/min → V = 0.1500 m^3
c) q =20 l/min → V = 0.2040 m^3.
In this case the ratio of hydrogen concentration after degassing to hydrogen concentration before degassing can be written as a function of equivalent bubble diameter. Combining equation (7) and equations (8) to (12), we can get the following relationship describing this ratio:

$$\frac{c_f}{c_i} = \exp\left(-0.011 \cdot \frac{\rho \cdot h}{M} \cdot \exp\left(-\frac{2969.16}{T}\right) \cdot d_e^{-1.75} \cdot V\right). \tag{13}$$

5. Experimental work and results

Refining of the AlSi7Mg alloy (0.18% Fe; 7.69% Si; 0.22% Mg) was carried out in IMN — OML Aluminium Foundry in Skawina with the use of reactors with stirring rotor URO — 200. The scheme of this rotor is presented in Fig. 6. Argon was used as a

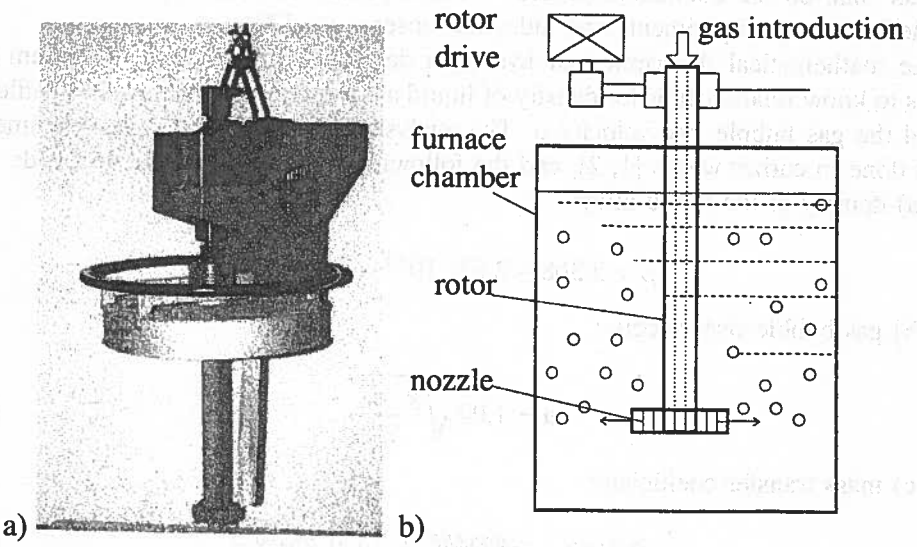

Fig. 6. a) Reactor URO — 200 using for the refining process of aluminium and its alloys b) the scheme of its working [24]

purge gas. The temperature of liquid alloy was 993 K. The height of liquid aluminium was 0.45 m. The batch of aluminium was melted in Monometer's resistance furnace of about 300 kg capacity. The refining process lasted 10 min, the flow rate of refining gas was in range from 10 through 15 to 20 dm^3/min. For these conditions the equivalent

gas bubble diameter was assumed as 0.005 to 0.0100 m. The hydrogen concentration in liquid metal was carried out using LECO RH 402 apparatus.

Table 1 presents the influence of flow rate of refining gas on the degassing process (final hydrogen concentration) and on the bubble gas diameter. The value of $c_{t(cal.)}$ which are the closest to experimental data are marked with grey color. This allowed us to estimate the bubble size at the determined value of flow rate of refining gas.
Assuming that the volume of refining gas is constant (12) we can use the equation (13) for the estimation the equivalent gas bubble diameter. For the alloy AlSi7Mg we can introduce into this equation the process parameters: M=300 kg, h=0.45 m, ρ=2352.2 kg/m^3, T = 993 K. After this operation this equation can be written in following form:

$$\frac{c_t}{c_i} = \exp(-0.00197 \cdot d_e^{-1.75} \cdot V). \tag{14}$$

TABLE 1

The influence of flow rate of refining gas on the aluminium degassing process and on the gas bubble diameter

Gas bubble diameter d, m	The flow rate of refining gas								
	q = 10 dm^3/min			q = 15 dm^3/min			q = 20 dm^3/min		
	c_i, cm^3/100g	c_t, cm^3/100g	$c_{t(calc.)}$, cm^3/100g	c_i, cm^3/100g	c_t, cm^3/100g	$c_{t(calc.)}$, cm^3/100g	c_i, cm^3/100g	c_t, cm^3/100g	$c_{t(calc.)}$, cm^3/100g
Melt 1									
0.0050	0.2912	0.0728	0.0360	0.2464	0.0840	0.0107	0.2688	0.0919	0.0041
0.0075			0.1043			0.0528			0.0345
0.0100			0.1564			0.0968			0.0775
Melt 2									
0.0050	0.3360	0.0560	0.0416	0.3250	0.0560	0.0142	0.3136	0.0784	0.0048
0.0075			0.1204			0.0697			0.0403
0.0100			0.1805			0.1276			0.0905
Melt 3									
0.0050	0.1792	0.0560	0.0222	0.1568	0.0448	0.0068	0.1568	0.0560	0.024
0.0075			0.0642			0.0336			0.0201
0.0100			0.0962			0.0616			0.0452
Melt 4									
0.0050	0.2576	0.0706	0.0319	0.1792	0.0762	0.0078	0.2016	0.0874	0.0031
0.0075			0.0923			0.0384			0.0259
0.0100			0.1384			0.0704			0.0582

Fig. 7 presents the ratio of final hydrogen concentration to initial hydrogen concentration calculated from equation (14) as a function of the equivalent gas bubble diameter

and the flow rate of refining gas. Basing on this we can estimate the value of the equivalent gas bubble diameter for the experimental hydrogen concentration from Table 1. Thus obtained values of these diameters are presented in Table 2.

TABLE 2

The equivalent gas bubble and its relations with the hydrogen concentration and the flow rate of refining gas in the refining process of AlSi7Mg alloy

The flow rate of refining gas								
q = 10 dm^3/min			q = 15 dm^3/min			q = 20 dm^3/min		
c_i, cm^3/100g	c_t, cm^3/100g	d_e, m	c_i, cm^3/100g	c_t, cm^3/100g	d_e, m	c_i, cm^3/100g	c_t, cm^3/100g	d_e, m
Melt 1								
0.2912	0.0728	0.0061	0.2464	0.0840	0.0087	0.02688	0.0919	0.0103
Melt 2								
0.3360	0.0560	0.0053	0.3250	0.0560	0.0068	0.3136	0.0784	0.0091
Melt 3								
0.1792	0.0560	0.065	0.1568	0.0448	0.0080	0.1568	0.0560	0.0106
Melt 4								
0.2576	0.0706	0.0062	0.1792	0.0762	0.0096	0.2016	0.0874	0.0115
Average value		0.0060	Average value		0.0083	Average value		0.0104

6. Discussion of results

At present the aluminium industry utilizes mainly the most popular are the refining reactors with impellers. In Poland this kind of reactors is represented by URO-200 unit constructed in IMN-OML in Skawina. This reactor is widely used in plants of aluminium products and semi- finished products.

The rate of degassing process is directly proportional to the interfacial contact area. If we know the gas bubble diameter and the bubble rise velocity we can estimate the interfacial contact area from the equation (8). In present calculations the equivalent bubble diameter was considered in the range 0.005 m to 0.010 m.

Basing on the compatibility of the values calculated from the mathematical model with the experimental results for the AlSi7Mg alloy we can claim that the values of final hydrogen concentration in industrial trials are in good agreement with calculated data. These results are presented in Table 1.

The gas bubble diameter has the great influence on the rate of the degassing process. In most cases this diameter is in range from 0.0050 m to 0.0075 m for the flow rate of refining gas equal q=10 dm^3/min. For the flow rate of refining gas equal to 15 dm^3/min the gas bubble diameter is slightly bigger, it is in range from 0.0075

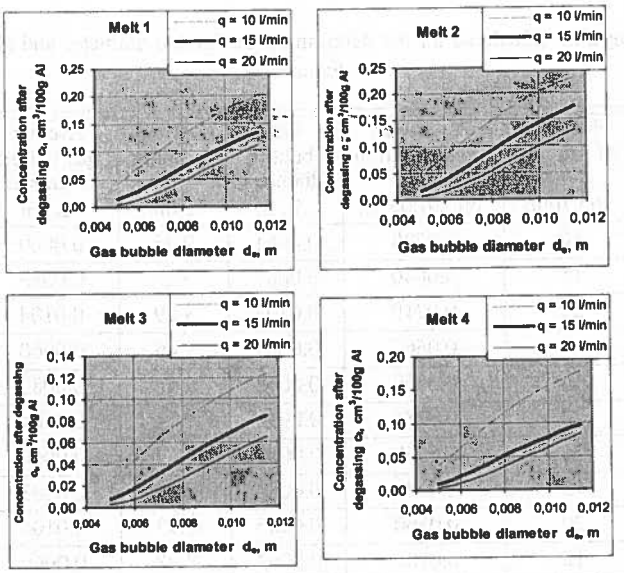

Fig. 7. The ratio of hydrogen removing from AlSi7Mg alloy as a function of the equivalent gas bubble diameter and the flow rate of refining gas

to 0.0100 m. This bubble diameter increases more strongly for the flow rate equal 20 dm^3/min, being about 0.0100 m or slightly more.

To facilitate estimation of the equivalent gas bubble diameter the assumption was made, that the volume of the refining gas introduced to the liquid alloy is constant. The equation (14) was based on this assumption. After the analysis of the obtained values of gas bubble diameter (Fig. 7, Table 2) we can claim that for the flow rate of refining gas equal to 10 dm^3/min the equivalent gas buble diameter is 0.0060 ± 0.00026 m, for the flow rate q = 15 dm^3/min this diameter is 0.0083 ± 0.00059 m, and for the flow rate of refining gas 20 dm^3/min the value of the equivalent gas bubble diameter is equal 0.0104 ± 0.00050.

In Table 3 the optimal refining time needed to obtain the experimental values of final hydrogen concentration basing on the estimated value of the equivalent gas bubble diameters and the average equivalent gas bubble diameter for the determined flow rate of refining gas were juxtaposed. It can be noticed that the optimal refining time is in range from 8 to 10 minutes for the determined gas bubble diameter and in the range from 7 to 14 minutes for the average equivalent gas bubble diameter. The value of the average optimal refining time for the determined gas bubble diameter is 9.02 ± 0.103, and for the average value of the equivalent gas bubble diameter 9.29 ± 0.600. According to this, the refining process of aluminium and its alloys can be conducted 10 minutes to obtain the desirable level of hydrogen concentration.

Basing on the analysis of the influence of the flow rate of refining gas on the rate of degassing process we can state that the higher the flow rate of refining gas,

TABLE 3

The optimal refining time calculated for the determined gas bubble diameter and also for their average diameter

Number of refining melt	Flow rate of refining gas q, dm^3/min	Hydrogen concentration c_t, cm^3/100g Al	Gas bubble diameter d_e, m	Optimal refining time t, min	Average gas bubble diameter d_e, m	Optimal refining time t, min
Melt 1	10	0.0728	0.0061	9.35	0.0060	9.09
	15	0.0840	0.0087	9.2	0.0083	8.31
	20	0.0919	0.0103	8.89	0.0104	9.04
Melt 2	10	0.0560	0.0053	9.45	0.0060	11.74
	15	0.0560	0.0068	9.58	0.0083	13.58
	20	0.0784	0.0091	9.24	0.0104	11.68
Melt 3	10	0.0560	0.0065	8.77	0.0060	7.62
	15	0.0448	0.0080	9.07	0.0083	9.67
	20	0.0560	0.0206	8.97	0.0104	8.67
Melt 4	10	0.0706	0.0062	8.98	0.0060	8.48
	15	0.0762	0.0096	8.52	0.0083	6.60
	20	0.0874	0.0115	8.39	0.0104	7.04
Average value				9.02	—	9.29

the better is the degassing process — at least in considered range of flow rate. The optimal level of flow rate of refining gas is between 10 to 15 dm^3/min. In this case the gas bubble diameter is about 0.005 to 0.010 m. The very close results we can get introducing the refining gas with the flow rate about 20 dm^3/min, but in this case the bubble diameter increases and the shape can be changed from spherical one through dimpled ellipsoidal cap, spherical cap to wobbling one (very deformed). There is also the danger of undesirable chain flow of refining gas what means that the dispersion would not be uniform (Fig. 8). For this reasons and economical one the flow rate of refining gas equal 20 dm^3/min is not desirable in industrial process.

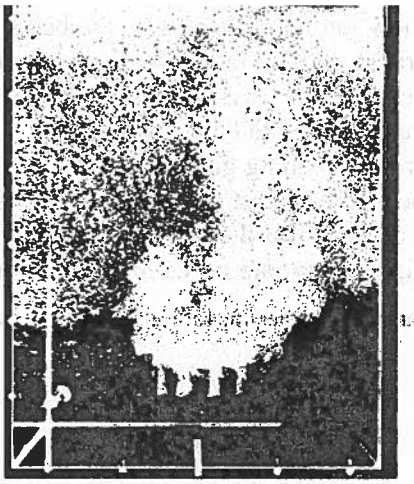

Fig. 8. The chain flow of refining gas (dispersion of refining gas in liquid metal is not uniform) — the flow rate of refining gas is 25 dm^3/min

7. Conclusions

The result of experiments which were carried out and the analysis of the flow rate of refining gas on the rate of degassing process let us draw the following conclusions:

— there is a good agreement between the result of industrial trials of refining the alloy AlSi7Mg and the calculated results from equation (7),

— assuming that the volume of refining gas introduced to the liquid alloy is constant equation (7) expresses the final hydrogen concentration as a function of the equivalent gas bubble diameter (13):

$$\frac{c_t}{c_i} = \exp\left(-0.011 \cdot \frac{\rho \cdot h}{M} \cdot \exp\left(-\frac{2969.16}{T}\right) \cdot d_e^{-1.75} \cdot V\right)$$

— for the 10 minutes refining process of AlSi7Mg alloy which processing parameters are the following: M=300 kg, h=0.45 m, ρ=2352.2 kg/m^3, T = 993 K, equation (13) can be written in the following form (14):

$$\frac{c_t}{c_i} = \exp(-0.00197 \cdot d_e^{-1.75} \cdot V)$$

— the calculated from equation (14) values of equivalent gas bubble diameter are respectively for the flow rate of refining gas:
- q = 10 dm^3/min: d_e = 0.0060 ± 0.00026 m,
- q = 15 dm^3/min: d_e = 0.0083 ± 0.00059 m,
- q = 20 dm^3/min: d_e = 0.0104 ± 0.00050 m.

— the optimal refining time is in the range from 8 to 10 minutes for the determined bubbles diameters, the average optimal time of refining process is 9.02 ± 0.103,

— the higher is the flow rate of refining gas, the better the degassing of metal is — at least in the range of flow rate used in this work:
  - optimal flow rate of refining gas is 10 to 15 dm^3/min, in this case the bubble diameter is in range: 0.005 to 0.010 m,
  - using the flow rate of refining gas equal 20 dm^3/min is not desirable: values of degassing process are almost the same like in the earlier flow rate, but there is the danger of the chain flow and the not uniform dispersion of gas. Moreover, the higher flow rate needs more refining gas.

Financial support from the Committee for Scientific Research (KBN) is acknowledged (contract No 7T08B 01921)

REFERENCES

[1] M. Saternus, Ph.D. Thesis, Politechnika Śląska, Katowice, (2002).
[2] M. Saternus, J. Botor, Rudy Metale **4**(48), 154-160 (2003).
[3] Z. Orzechowski, Przepływy dwufazowe, PWN, Warszawa (1990).
[4] R. Clift, J.R. Grace, M.E. Weber, Bubbles, Drops and Particles, Academic Press, New York (1978).
[5] J. Botor, Prace IMN Dodatek **7**(1), 3-40 (1978).
[6] D.W. Van Krevelen, P.J. Hoflizjer, Chem. Eng. Progr. **46** (1950).
[7] C.G. Maier, U.S. Bur. Mines Bull. (1927).
[8] R.J. Benzig, J.E. Myers, Ind. Eng. Chem. **47**, (1955).
[9] A. Mersen, VDI Forshungsheft **491** (1962).
[10] L. Davidson, E.H.Jr. Amick, AIChE Journal **2**, 337 (1956).
[11] I. Leibson, E.G. Halcomb, A.G. Cacoso, J.J. Jacmic, AIChE Journal 2, 296 (1956).
[12] J. Botor, Podstawy metalurgicznej inżynierii procesowej, Wydawnictwo Politechniki Śląskiej, Gliwice (1999).
[13] J.Y. Oldshue, Chemical Engineering, McGraw-Hill, (1983) w J.J.J. Chen, J.C. Zhao, Light Metals 1227 (1995).
[14] Sprawozdanie IMN- OML, Nr 5100/III/95, Skawina (1995).
[15] R.D. Pehlke, A.I. Bement, Trans. AIME **224**, 1237 (1962).
[16] J. Botor, Prace IMN 10 (2), 58 (1981).
[17] G.K. Sigworth, T.A. Engh, Metall. Trans. **13B**, 447 (1982).
[18] T.A. Engh, Principles of Metal Refining, Oxford University Press, Oxford, 1, (1992).
[19] D.E.J. Talbot, D.A. Granger, J.Inst. Metals **92**, 290 (1963-64).
[20] J. Benavides, G.I. Senel, M.C. Flemings, J.W. Tester, A.F. Sarofim, Metall. Mater. Trans. **32B**, 285 (2001).
[21] M. Nilmani, P.K. Thay, C.J. Simensen, Light Metals, TMS 939 (1992).
[22] P. Waite, R. Thiffault, Light Metals 1001 (1996).
[23] J. Botor, H. Palut, Prace IMN **5**(3), 131 (1976).
[24] Sprawozdanie IMN-OML Nr 1864012, Skawina (2002).

Received: 20 October 2005.